J. Anat. (2018) **233**, pp193–203 doi: 10.1111/joa.12830

Effects of selective breeding for high voluntary wheel-running behavior on femoral nutrient canal size and abundance in house mice

Nicolas L. Schwartz,[1,2] Biren A. Patel,[3] Theodore Garland Jr[2] and Angela M. Horner[1]

[1]*Department of Biology, California State University San Bernardino, San Bernardino, CA, USA*
[2]*Department of Evolution, Ecology, and Organismal Biology, University of California, Riverside, Riverside, CA, USA*
[3]*Department of Integrative Anatomical Sciences and Department of Biological Sciences, University of Southern California, Los Angeles, CA, USA*

Abstract

Bone modeling and remodeling are aerobic processes that entail relatively high oxygen demands. Long bones receive oxygenated blood from nutrient arteries, epiphyseal-metaphyseal arteries, and periosteal arteries, with the nutrient artery supplying the bulk of total blood volume in mammals (~ 50–70%). Estimates of blood flow into these bones can be made from the dimensions of the nutrient canal, through which nutrient arteries pass. Unfortunately, measuring these canal dimensions non-invasively (i.e. without physical sectioning) is difficult, and thus researchers have relied on more readily visible skeletal proxies. Specifically, the size of the nutrient artery has been estimated from dimensions (e.g. minimum diameters) of the periosteal (external) opening of the nutrient canal. This approach has also been utilized by some comparative morphologists and paleontologists, as the opening of a nutrient canal is present long after the vascular soft tissue has degenerated. The literature on nutrient arteries and canals is sparse, with most studies consisting of anatomical descriptions from surgical proceedings, and only a few investigating the links between nutrient canal morphology and physiology or behavior. The primary objective of this study was to evaluate femur nutrient canal morphology in mice with known physiological and behavioral differences; specifically, mice from an artificial selection experiment for high voluntary wheel-running behavior. Mice from four replicate high runner (HR) lines are known to differ from four non-selected control (C) lines in both locomotor and metabolic activity, with HR mice having increased voluntary wheel-running behavior and maximal aerobic capacity (VO_2max) during forced treadmill exercise. Femora from adult mice (average age 7.5 months) of the 11th generation of this selection experiment were μCT-scanned and three-dimensional virtual reconstructions of nutrient canals were measured for minimum cross-sectional area as a skeletal proxy of blood flow. Gross observations revealed that nutrient canals varied far more in number and shape than prior descriptions would indicate, regardless of sex or genetic background (i.e. HR vs. C lines). Canals adopted non-linear shapes and paths as they traversed from the periosteal to endosteal borders through the cortex, occasionally even branching within the cortical bone. Additionally, mice from both HR and C lines averaged more than four nutrient canals per femur, in contrast to the one to two nutrient canals described for femora from rats, pigs, and humans in prior literature. Mice from HR lines had significantly larger total nutrient canal area than C lines, which was the result not of an increase in the number of nutrient canals, but rather an increase in their average cross-section size. This study demonstrates that mice with an evolutionary history of increased locomotor activity and maximal aerobic metabolic rate have a concomitant increase in the size of their femoral nutrient canals. Although the primary determinant of nutrient canal size is currently not well understood, the present results bolster use of nutrient canal size as a skeletal indicator of aerobically supported levels of physical activity in comparative studies.

Correspondence
Nicolas L. Schwartz, Department of Evolution, Ecology, and Organismal Biology, University of California, Riverside, Riverside, CA 92521, USA.
T: + 1 951 8273524; F: + 1 951 8274286; E: nschw002@ucr.edu

Accepted for publication *27 April 2018*
Article published online *31 May 2018*

Key words: artificial selection; behavior; evolutionary morphology; exercise; femur; *Mus domesticus*; nutrient canal; voluntary wheel running.

Introduction

Although the vertebrate skeleton is composed of rigid, mineralized tissue, bone is dynamic, responding to changing mechanical needs during growth, load bearing, and locomotion (Frost, 1987). Bone modeling and remodeling in response to exercise is well documented (Rubin & Lanyon, 1984; Eliakim et al. 1997; Lieberman, 2003; Rector et al. 2008; Katsimbri, 2017). However, the skeleton's response to loading varies in relation to age (e.g. Pearson & Lieberman, 2004), hormones (e.g. Devlin & Lieberman, 2007), sex (e.g. Robling et al. 2007), exercise frequency (e.g. Rubin & Lanyon, 1984), and exercise magnitude (e.g. Rector et al. 2008). Additionally, differences in skeletal morphology may be a result of genetic variation among individuals, an effect that is rarely accounted for (Middleton et al. 2008; Wallace et al. 2010, 2012).

Variations in skeletal morphology, whether caused by inherent genetic differences among individuals or plastic responses to physical activity and other factors, are achieved by the opposing processes of bone deposition and resorption, via osteoblasts and osteoclasts, respectively. These bone cells are highly aerobic, exhibiting metabolic rates comparable to those of tissues in the nervous system (Schirrmacher et al. 1997). As a result, osteoblast and osteoclast activity are a major source of oxygen consumption within bone (Knothe Tate, 2003), and their activity contributes to the overall aerobic metabolic rate of an organism (Schirrmacher et al. 1997). Increases in bone cell activity (e.g. in response to exercise) necessitate increased blood flow to the skeleton (Sim & Kelly, 1970; Gross et al. 1981). The long bones of amniotes receive blood from three sources – nutrient arteries, epiphyseal-metaphyseal arteries, and periosteal arteries (Rhinelander, 1972) – with the nutrient artery accounting for ~ 50–70% of total blood supply for the cortical and medullary regions (Trueta, 1964).

As the cellular activity of a bone increases, an increase in blood perfusion must occur (Sim & Kelly, 1970; Gross et al. 1981), and the resultant increase in arterial vessel size is expected to be visible in the dimensions of the nutrient foramen (Seymour et al. 2012). Prior literature on nutrient arteries and their foramina is limited to anatomical descriptions, suggesting that a single nutrient artery enters the diaphysis of long bones by perpendicularly penetrating the cartilaginous primordium during bone formation. The ensuing asymmetrical growth of long bones results in the nutrient foramen of adults being neither centrally placed nor at a right angle to the long axis of the bone, but rather developing an oblique orientation (Greene, 1935; Rogers & Gladstone, 1950; Brookes & Harrison, 1957; Brookes, 1958; Henderson, 1978). The nutrient artery does not appear to branch within the nutrient canal but does branch upon passing the endosteal border and breaching into the medullary cavity, approaching the metaphyseal ends of the bone (Singh et al. 1991). Arteries of medullary vessels end in medullary sinusoids, which drain into a central venous channel. The central vein of these channels retraces the path of the nutrient artery out of the bone, though they may also exit independently (Brookes, 1971).

A few recent studies have investigated the potential link between nutrient foramen structure and organismal physiology (Seymour et al. 2012; Allan et al. 2014). These studies have suggested that the size of the external (i.e. periosteal) opening of the nutrient foramen is a suitable proxy for aerobic maximal metabolic rate. However, the oblique shape of the nutrient foramen, coupled with the inability to determine visually the direction of the nutrient canal through the cortex from the external surface of bone, prevents accurate determination of nutrient foramen size based on external dimensions alone; that is, non-perpendicular measurements of ovoid-shaped openings could cause error in assessing true diameters. Additionally, these studies have presumed that the nutrient foramen is the location with the minimum cross-sectional area [i.e. the region where size would limit blood flow as described by the Hagen–Poiseuille equation: $Q = (P\pi r^4)/(8L\eta)$, where Q is flow rate, P is the difference in blood pressure, L is vessel segment length, η is blood viscosity, and r is the radius of the vessel] of the nutrient canal, despite no prior observations as as to whether the canal widens or narrows from the periosteal surface to the endosteal surface. As a result, the existing link between nutrient foramen size and maximal metabolic intensity (Seymour et al. 2012; Allan et al. 2014) requires additional verification, ideally using methods which account for the orientation of the nutrient foramen and the ability to measure the minimum cross-sectional area along the entire length of the nutrient canal through the bone cortex. Studies that describe nutrient arteries and their foramina have been scarce, and no studies to date have accurately modeled both the size and shape of nutrient canals.

Before investigating potential links between nutrient canals and physiological traits, a more realistic representation of nutrient canals and the ability to measure nutrient canal size are needed. Therefore, a primary objective of the present study is to document nutrient canal abundance and size in femora using three-dimensional (3D) virtual methods. In addition, we test whether nutrient canal size is an appropriate indicator of physical or metabolic activity using a well-established model system: mice from four replicate high runner (HR) lines that have been selectively bred for voluntary wheel-running behavior and their four

non-selected Control (C) lines (Swallow et al. 1998a; Garland, 2003). Mice from the HR lines run approximately threefold more revolutions per day than C mice, and also have higher maximum aerobic capacity (VO_2max) and endurance during forced treadmill exercise (Swallow et al. 1998b; Girard et al. 2001; Rezende et al. 2006a,b; Meek et al. 2009; Kolb et al. 2010; Dlugosz et al. 2013). If metabolic activity impacts nutrient canal dimensions, then more active individuals, populations and species are predicted to have relatively larger canals (Seymour et al. 2012), and this should be reflected in differences between the HR and C lines of mice.

Methods

Laboratory house mice (*Mus domesticus*) from a long-term artificial selection experiment on voluntary wheel-running behavior were used for this study (Swallow et al. 1998a; Garland, 2003). These mice originated from a base population of the outbred Hsd:ICR stock. Each generation of 6- to 8-week-old mice was housed individually with access to Wahman-type activity wheels (1.12-m circumference) for 6 days, and daily revolutions were recorded with a computer-automated system in 1-min bins. For each of four replicate HR lines, the highest-running male and female on days 5 and 6 of the 6-day trial were chosen from within each of 10 families to provide breeders to produce the next generation, with no sibling matings allowed. For each of the four C lines, the procedure was similar, except that breeders were chosen randomly from within each family.

Two of the HR lines and one of the C lines were observed to have individuals with hindlimb muscles that were reduced by ~ 50% as compared with normal-muscle individuals (Garland et al. 2002; Houle-Leroy et al. 2003). This 'mini-muscle' phenotype is caused by an autosomal, Mendelian-recessive, single nucleotide polymorphism (Kelly et al. 2013). The mini-muscle phenotype was originally present at low frequency in the base population and has increased in frequency in subsequent generations in both HR lines (Garland et al. 2002), resulting in fixation in HR line 3 and ~ 50% frequency in HR line 6 (Syme et al. 2005). Pleiotropic effects of this condition relevant to the present study include higher average running speeds on wheels (Dlugosz et al. 2009), higher maximal aerobic capacity in hypoxia (Rezende et al. 2006a) and sometimes during normoxia (Hiramatsu et al. 2017), reduced hind limb bone diaphyseal diameters and reduced femoral polar moments of area and cortical areas (Kelly et al. 2006; Wallace et al. 2012). In the present sample of 137 mice, eight mice had the mini-muscle phenotype: six were present in HR line 3 (four males, two females) and two were present in HR line 6 (one male, one female).

Femora from mice of generation 11 of the selection experiment were used. These mice had previously been measured in another study, where measures of body size were recorded and femoral morphometrics were taken with digital calipers (Garland & Freeman, 2005). Mice were sacrificed via carbon dioxide at 232 days of age and defleshed via a dermestid beetle colony. The right femur of each mouse was scanned with an isometric voxel resolution of 10 μm using a SCANCO μCT 50 specimen scanner (SCANCO Medical) housed in the Molecular Imaging Center at the University of Southern California. Other scanner parameters included: energy: 70 kV; current: 60 μA; exposure time: 300 ms; filter: 0.5 mm aluminum. Three to five femora were scanned simultaneously to expedite the scanning of 137 specimens. Each femur was scanned as close to vertical in orientation such that the long axis of its diaphysis was near perpendicular to the scanning plane. Prior to analysis, each femur was isolated into its own image stack. The raw data were reconstructed as 16-bit DICOM images and these sequential slices were imported into AMIRA 5.6 software (FEI) for visualization, segmentation, and analysis. Using the AMIRA *Isosurface* module, surface renderings of the femur were created to inspect the external morphology for nutrient foramen (defined as a superficial opening through which the nutrient artery passes) restricted to the portion of bone inferior to the femoral neck and superior to the proximal edge of the patellar groove (Fig. 1). This restricted range was implemented to ensure only nutrient vessels were examined, as metaphyseal and epiphyseal blood vessels typically penetrate bone outside of this region. To confirm whether a nutrient foramen was correctly identified, The AMIRA *OrthoSlice* module was used to inspect sequential transverse slices superior and inferior to each external opening. The identification of a nutrient canal (defined as a tubular duct housing the nutrient artery) was ultimately accepted if there was a continuous absence of cortical bone from the periosteal (external) border of the cortex, traversed through the cortex towards the medullary cavity, and ultimately past the endosteal surface (Fig. 2). Upon identification, the empty space of the nutrient canal was manually segmented out slice by slice in AMIRA (Fig. 2) and a 3D surface model was created of the isolated nutrient canal using the *Label Field* module (Fig. 3). Each canal was then isolated from the femur and virtually re-oriented using the *Align Principal Axes* function such that a transverse cross-section could be obtained perpendicular to the long axis of the canal (Fig. 3). Reorienting was necessary so that elliptical cross-sections could be avoided, as they have the potential to overestimate area compared with a more circular shape. Multiple transverse cross-sections spanning the length of the reoriented canal were measured for area, with only the minimum cross-sectional area being recorded for subsequent analyses. The minimum cross-sectional area was chosen because flow is limited by the smallest sectional area in a cylindrical pipe as described

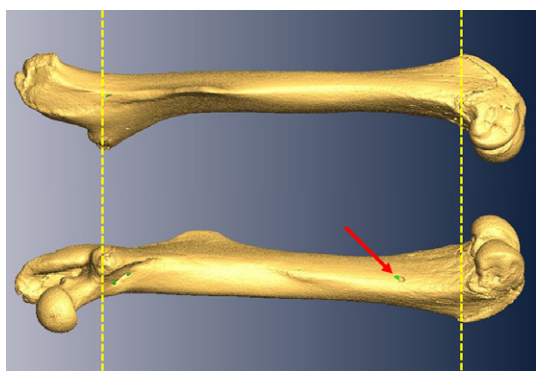

Fig. 1 Virtual rendering derived from μCT scans of a representative mouse femur from the HR line. The top image shows a lateral view of the femur and the bottom image shows a medial view. In each, to the left is proximal and to the right is distal. Red arrow denotes the presence of a nutrient foramen (green dots) in the distal third of the femur. All measurements were restricted to the region above the patellar groove and below the base of the femoral neck (as indicated by the yellow dashed lines) to prevent inclusion of metaphyseal and periosteal vessels which frequently penetrate bone outside this defined area.

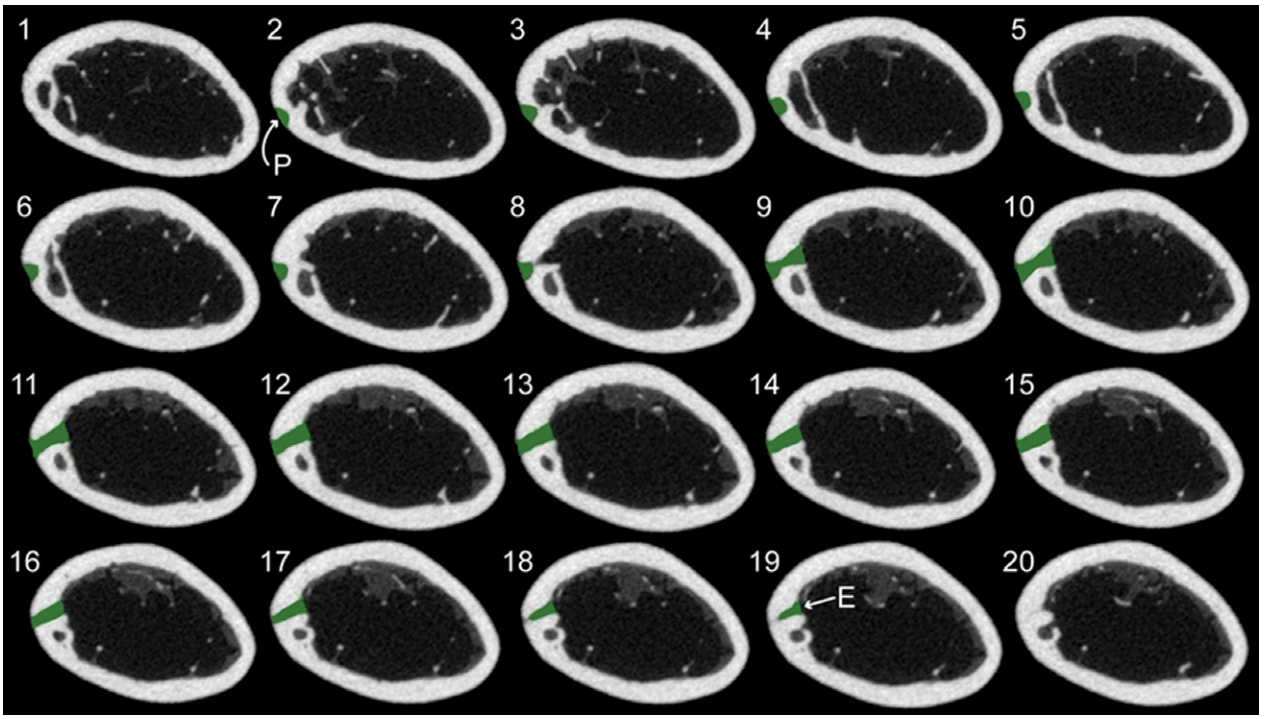

Fig. 2 Sequential transverse slices of a mouse femur from proximal (slice #1, upper left) to distal (slice #20, bottom right) showing the nutrient canal (highlighted in green) from the outer periosteal surface (indicated with a P) to inner endosteal surface (E).

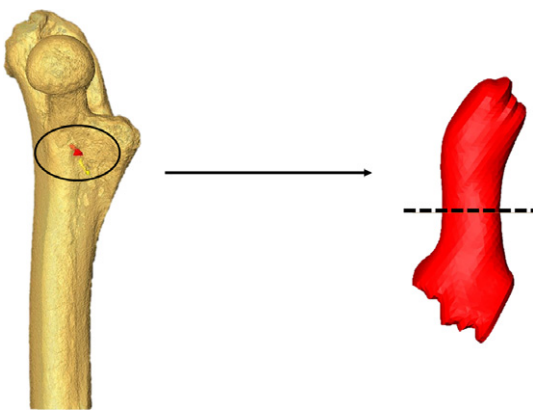

Fig. 3 Left: a transparent rendering of the proximal half of a mouse femur illustrating a segmented nutrient canal (red) *in situ*. Right: isolated nutrient canal that has been virtually re-oriented so that the principal axis of the canal is positioned vertically to facilitate obtaining a perpendicular mid-canal cross-section (shown with the dashed line).

by the Hagen–Poiseuille equation: $Q = (P\pi r^4)/(8L\eta)$, where Q is flow rate, P is the difference in blood pressure, L is vessel segment length, η is blood viscosity, and r is the radius of the vessel.

In the process of modeling nutrient canals, it became clear that they differed in size and shape more than would be expected based on prior literature (e.g. Singh et al. 1991). Often the canal would adopt a non-linear or curved shape in its path from the periosteal surface to the medullary cavity (Fig. 4). To ensure the minimum cross-sectional area of each canal was being measured, and overestimation caused by measuring at an oblique angle was minimized, the long axis of the canal was reoriented several times along the canal length at each major inflection point (assessed visually) such that multiple perpendicular cross-sections could be obtained (Supporting Information Fig. S1). From these sets of cross-sections along the curved canal, only the one with the smallest cross-sectional area was used in any further analyses.

Additionally, we noticed during that nutrient canals occasionally branched one or more times within the cortical bone (Fig. 4). When this occurred, all potential branches were measured for minimum cross-sectional area in accordance with the methods described above (Supporting Information Fig. S2). If the sum of the minimum cross-sectional areas of the branches was greater than their source trunk, then the branches were not considered to be blood flow-limiting structures and were ignored and only the trunk was recorded. If the cross-sectional area of the source trunk was greater than the sum of its branches, then the branches were the blood flow-limiting structures and both branches counted as distinct nutrient canals, and the trunk was ignored (Fig. S2). In addition to the minimum cross-sectional area of each nutrient canal, the total number of canals and their location (proximal or distal) on the femur were recorded to determine the abundance of nutrient canals.

All statistical analyses were performed using SAS PROCEDURE MIXED v. 12. Comparisons were made for the proximal region and distal region, and for the proximal and distal regions combined (i.e. total) for both area measurements and counts. C and HR lines were compared by a two-way (linetype, sex) mixed-model nested analysis of covariance, with line as a random effect nested within linetype, and body length, body mass, and femoral length tested as potential covariates, based on prior studies demonstrating that these traits correlated with femoral morphometrics (Kelly et al. 2006; Middleton et al. 2008; Seymour et al. 2012). A main effect of the mini-muscle phenotype was also included, as mini-muscle individuals are

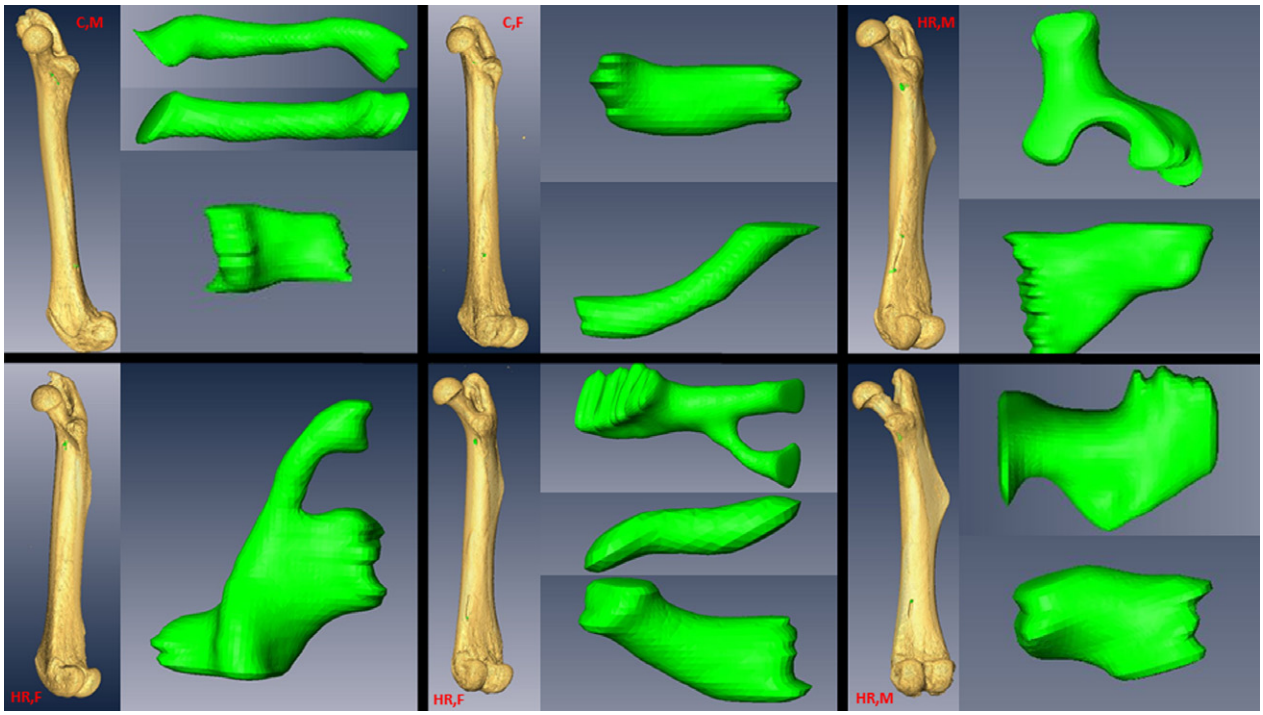

Fig. 4 Representative virtual renderings of nutrient canals across a sample of mice in this study. Note the complexity including simple linear canals, simple curved canals, bifurcating canals, blocky canals, and widening canals.

known to differ in femoral morphology (Kelly et al. 2006). Statistical significance was judged at $P < 0.05$. Data on nutrient canal area were square root-transformed to normalize residuals, but this was unnecessary for canal numbers. Least-squares (adjusted) means and standard errors for dependent variables were taken from SAS PROCEDURE MIXED.

Results

No significant effects of linetype were detected for body mass, body length or femur length ($P = 0.23$, $P = 0.48$, $P = 0.69$, respectively, Table 1). Sex effects were detected for body mass and femur length, with males being significantly heavier and possessing shorter femora than females ($P < 0.0001$, $P = 0.0007$, Table 1). Additionally, a significant effect of the mini-muscle phenotype was detected for body mass, with mini-muscle mice being significantly lighter than mice without the phenotype ($P = 0.0297$, Table 1).

Body mass, body length, and femur length were identified as potential covariates in early analyses; however, none of these covariates was statistically significant for any

Table 1 Results from two-way nested analysis of variance for body mass, body length, and femur size, along with least square means (± standard errors) from SAS PROCEDURE MIXED.

		Linetype effects			Sex effects			Linetype × Sex			Mini-muscle effects		
Variable	*n*	df	*F*	*P*	df	*F*	*P*	df	*F*	*P*	df	*F*	*P*
Body mass	136	1, 6	1.76	0.2326	1, 6	**201.85**	**< 0.0001**	1, 6	0.75	0.4205	1, 119	**4.84**	**0.0297**
Body length	140	1, 6	0.54	0.4899	1, 6	0.00	0.9914	1, 6	0.68	0.4411	1, 123	0.39	0.5342
Femur length	139	1, 6	0.17	0.6905	1, 6	**40.89**	**0.0007**	1, 6	0.55	0.4878	1, 122	2.71	0.1024

		Control		High runner			
Variable	*n*	Male	Female	Male	Female	Normal	Mini-muscle
Body mass (g)	136	44.51 ± 1.45	33.94 ± 1.49	41.80 ± 1.35	32.44 ± 1.41	39.99 ± 0.79	36.35 ± 1.75
Body length (mm)	140	113.20 ± 1.13	112.72 ± 1.15	111.85 ± 1.05	112.32 ± 1.10	112.94 ± 0.60	112.10 ± 1.40
Femur length (mm)	139	15.75 ± 0.19	16.25 ± 0.19	15.71 ± 0.18	16.10 ± 0.19	16.09 ± 0.12	15.82 ± 0.19

Significant values ($P < 0.05$) are in bold.

canal trait measured (Supporting Information Table S1) and thus they were excluded from final analyses. As already noted above, nutrient canals were far more variable in number, size, and structure than predicted from prior literature (Fig. 4).

Effects of selective breeding

Mice from the HR lines had significantly higher total cross-sectional area of canals than those from C lines ($P = 0.0304$, Fig. 5E, Table 2), attributable mainly to higher proximal canal cross-sectional area ($P = 0.0434$, Fig. 5A, Table 2) rather than distal canal cross-sectional area ($P = 0.15$, Fig. 5C, Table 2). Larger cross-sectional area observed in HR lines was not attributable to increases in the number of canals, as no significant differences in canal number were detected in either the proximal ($P = 0.29$, Fig. 6A, Table 2) or distal regions ($P = 0.49$, Fig. 6C, Table 2), or in the total number of canals ($P = 0.25$, Fig. 6E, Table 2).

Effects of sex

Male mice tended to have higher total cross-sectional area of canals than females ($P = 0.0515$, Fig. 5E, Table 2), driven by a significant difference in distal canal cross-sectional area ($P = 0.0491$, Fig. 5C, Table 2), but not by differences in proximal canal cross-sectional area ($P = 0.22$, Fig. 5A, Table 2). The higher canal cross-sectional area observed in male mice was not caused by increases in the number of canals, as no significant differences in nutrient canal number were detected in the proximal ($P = 0.42$, Fig. 6A, Table 2) or distal regions ($P = 0.90$, Fig. 6C, Table 2), or in total canal number ($P = 0.56$, Fig. 6E, Table 2).

Effects of the mini-muscle phenotype

Distal canal cross-sectional area was the only variable significantly affected by the presence of the mini-muscle phenotype, with mini-muscle individuals having higher distal canal cross-sectional area than normal mice ($P = 0.0488$, Fig. 5D, Table 2). This increase in distal canal cross-sectional area was accompanied by a trend for mini-muscle mice to have more distal canals than normal mice ($P = 0.0752$, Fig. 6D, Table 2). No significant differences of the mini-muscle phenotype were detected in proximal canal cross-sectional area ($P = 0.98$, Fig. 5B, Table 2) or number ($P = 0.54$, Fig. 6B, Table 2), or in total cross-sectional area

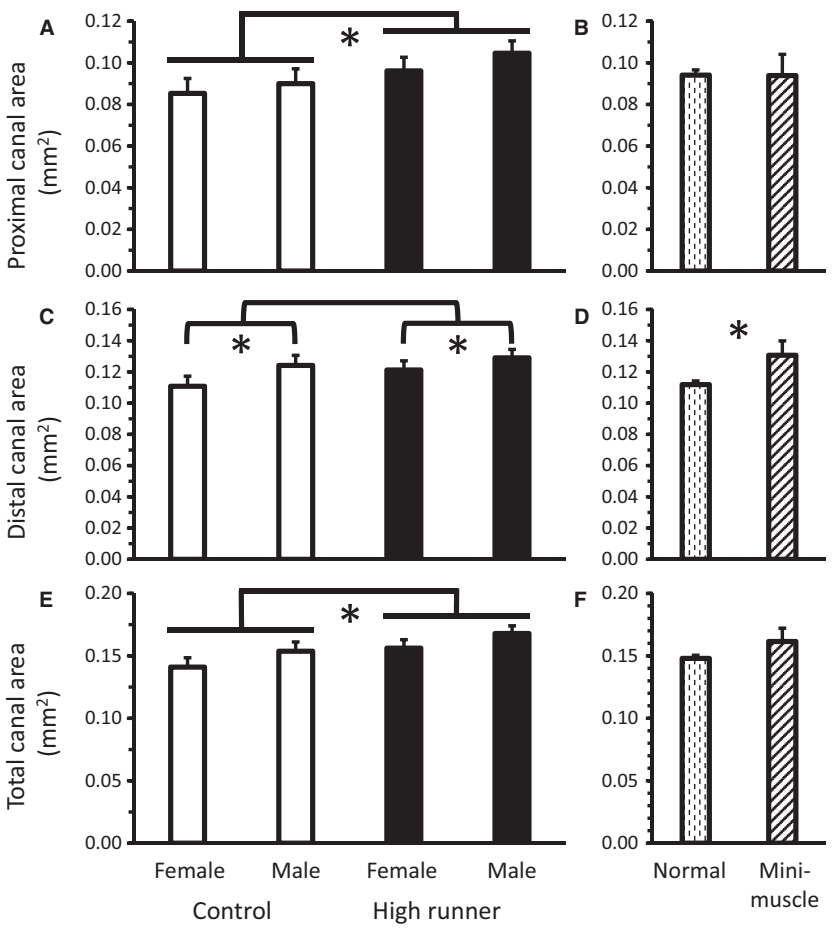

Fig. 5 Average minimum cross-sectional area of nutrient canals (least squares means ± standard error) present in the (A) proximal ($n = 133$: one individual with no proximal canals), (C) distal ($n = 134$), and (E) total ($n = 134$) of the diaphysis for male and female mice of HR (black bars) and C lines (white bars). (A) HR mice had a higher proximal canal area than C mice. (C) Male mice had higher distal canal area than female mice. (E) HR mice had a higher total canal area than C mice. Average minimum cross-sectional area (least squares means ± standard error) of nutrient canals present in the (B) proximal, (D) distal, and (F) entire diaphysis for mice without (dashed bars) vs. with the mini-muscle (striped bars) phenotype. (D) Mice with the mini-muscle phenotype had a higher distal canal area than mice without the phenotype. Significant differences ($P < 0.05$) are indicated with an asterisk.

Table 2 Results from two-way nested analysis of variance of nutrient canal dimensions and counts, along with least square means (± standard errors) from SAS PROCEDURE MIXED.

		Selection effects			Sex effects			Sex × Linetype			Mini-muscle effects		
Variable	*n*	df	*F*	*P*	df	*F*	*P*	df	*F*	*P*	df	*F*	*P*
Proximal area (mm^2)	133	1, 6	**6.51**	**0.0434**	1, 6	1.86	0.2215	1, 6	0.16	0.7065	1, 116	0	0.9857
Distal area (mm^2)	134	1, 6	2.69	0.1522	1, 6	**6.05**	**0.0491**	1, 6	0.42	0.5396	1, 117	**3.97**	**0.0488**
Total area (mm^2)	134	1, 6	**7.94**	**0.0304**	1, 6	5.88	0.0515	1, 6	0.01	0.9233	1, 117	1.55	0.2158
Proximal number	137	1, 6	1.32	0.2941	1, 6	0.72	0.4278	1, 6	0.83	0.3969	1, 120	0.38	0.5407
Distal number	137	1, 6	0.53	0.4924	1, 6	0.01	0.9068	1, 6	1.28	0.3003	1, 120	3.22	0.0752
Total number	137	1, 6	1.58	0.2560	1, 6	0.38	0.5622	1, 6	1.96	0.2115	1, 120	2.69	0.1033

		Control		High runner			
Variable	*n*	Male	Female	Male	Female	Normal	Mini-muscle
Proximal area (mm^2)	133	0.0899 ± 0.0071	0.0852 ± 0.0071	0.1046 ± 0.0059	0.0961 ± 0.0065	0.0940 ± 0.0024	0.0939 ± 0.0101
Distal area (mm^2)	134	0.1242 ± 0.0064	0.1108 ± 0.0065	0.1290 ± 0.0054	0.1212 ± 0.0059	0.1119 ± 0.0023	0.1307 ± 0.0091
Total area (mm^2)	134	0.1537 ± 0.0073	0.141 ± 0.0075	0.1678 ± 0.0062	0.1561 ± 0.0068	0.1479 ± 0.0025	0.1615 ± 0.0106
Proximal number	137	2.069 ± 0.1585	2.062 ± 0.1606	1.842 ± 0.1347	2.033 ± 0.1467	1.930 ± 0.0557	2.073 ± 0.2273
Distal number	137	2.531 ± 0.2480	2.361 ± 0.2513	2.214 ± 0.2099	2.425 ± 0.2291	2.052 ± 0.0864	2.714 ± 0.3580
Total number	137	4.905 ± 0.3437	4.723 ± 0.3483	4.279 ± 0.2910	4.747 ± 0.3176	4.243 ± 0.1198	5.084 ± 0.4962

Significant values ($P < 0.05$) are in bold.

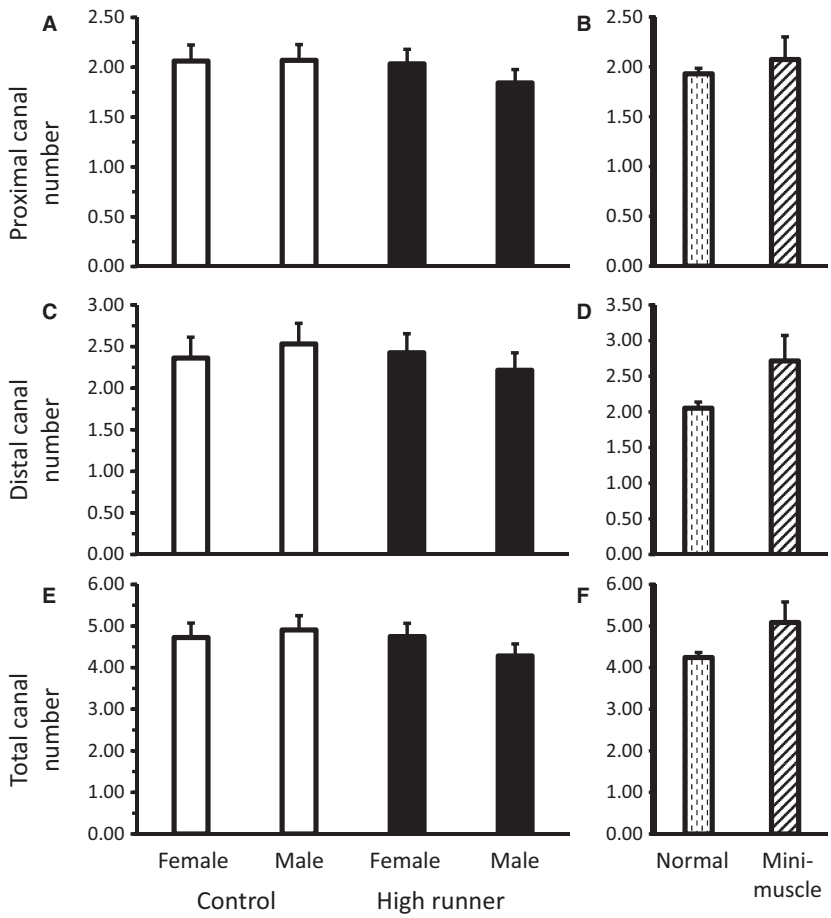

Fig. 6 Average count of nutrient canals (least squares means ± standard error) present in the (A) proximal (n = 137), (C) distal (n = 137), and (E) total (n = 137) diaphysis for male and female mice of HR (black bars) and C lines (white bars). Average number (least squares means ± standard error) of nutrient canals present in the (B) proximal, (D) distal, and (F) total diaphysis for mice without vs. with the mini-muscle phenotype. No significant differences were found in comparisons.

($P = 0.21$, Fig. 5F, Table 2) or number ($P = 0.10$, Fig. 6F, Table 2).

Discussion

Effect of selective breeding for wheel running on nutrient canals

Mice from HR and C lines used in the present study had statistically similar body mass, body length, and femoral length (Table 1), consistent with previous reports for mice from generations 10 and 11 of the selection experiment (Swallow et al. 1998b; Castro & Garland, 2018). In subsequent generations, however, HR mice have evolved to be significantly smaller in body mass (Swallow et al. 1999, 2001) and body length (Kelly et al. 2006), accompanied by lower post-weaning growth rates (Girard & Garland, 2002; Malisch et al. 2006). Although prior studies have demonstrated the importance of controlling for size-related variables when examining femoral morphology (Middleton et al. 2008; Seymour et al. 2012), nutrient canal cross-sectional area and number varied independently of the metrics of body size examined here (Table S1).

High runner mice have increased activity levels, displaying higher voluntary-wheel running behavior than C mice in generations prior and subsequent to the generation studied here (Swallow et al. 1998a; Meek et al. 2009). HR mice run more revolutions per day than C counterparts and this increase in wheel running is attributable primarily to an increase in running speed rather than an increase in overall time spent running (Swallow et al. 1998a; Garland et al. 2011). Additionally, at least in later generations, HR mice also have elevated home-cage activity when housed without wheels (Malisch et al. 2009; Copes et al. 2015). As a result of the selection applied, HR mice also have a higher maximal rate of oxygen consumption during forced treadmill exercise (VO_2max) (Swallow et al. 1998b; Rezende et al. 2006a,b; Kolb et al. 2010; Dlugosz et al. 2013).

High runner mice have a concomitant increase in the minimum cross-sectional area of their femoral nutrient canals (Fig. 5E, Table 2). This increase is not the result of increases in nutrient canal number (Fig. 6E, Table 2), although both HR and C mice have more nutrient canals than would be expected based on prior literature (addressed below) (Payton, 1934; Carroll, 1963; Campos et al. 1987). Any blood vessels supplying the skeleton are limited in maximum size by the surrounding bone, and thus nutrient canals are expected to accommodate maximal blood flow (Seymour et al. 2012). However, whether blood flow through nutrient arteries is determinant of bone morphology (i.e. blood flow dictates bone size and/or structure) or bone metabolic need determines blood flow through the nutrient artery (i.e. osteoblast/osteoclast bone activity dictate blood flow to bone) is currently unclear. Additionally, the size of long bone nutrient canals may be related to multiple factors. In terms of function, larger canals would allow greater maximal rates of blood flow. In turn, higher rates of blood flow might allow more rapid skeletal growth rates (Trueta, 1964; Carano & Filvaroff, 2003), more rapid modeling and remodeling (Sim & Kelly, 1970), and more rapid fracture repair (Trueta, 1974; Carano & Filvaroff, 2003). Although it is not clear which of these, if any, causes maximal blood flow to long bones, bone is a highly aerobic tissue (Schirrmacher et al. 1997) and has a large blood flow volume, with an estimated 11% of total cardiac output being directed towards the skeleton at rest (Gross et al. 1981).

Effect of sex on nutrient canals

In addition to an effect of selective breeding, we found that males tended to have a higher minimum cross-sectional area of their femoral nutrient canals than females (Fig. 5E, Table 2). Female mice exhibit higher voluntary wheel-running behavior than males in terms of total distance run, average running speed, and time spent running (Swallow et al. 1998a; Garland et al. 2011). However, male mice appear to have increased VO_2max compared with females (Rezende et al. 2006a), introducing the possibility that the sex differences in nutrient canal area are associated more with VO_2max than running behavior *per se*. Further study would be needed to differentiate sex-related variation in nutrient canal size from variation related to maximal metabolic rate and locomotor activity.

Effect of the mini-muscle phenotype on nutrient canals

Mini-muscle mice are distinct in several ways from other mice of the selection experiment; for example, mini-muscle mice have much smaller hindlimb muscles, but enlarged livers, kidneys, and ventricular heart masses (Garland et al. 2002), elongated femoral length (Kelly et al. 2006), and increased mass-specific mitochondrial enzyme activity in hindlimb muscle (Houle-Leroy et al. 2003). However, mini-muscle variants probably did not differ from normal mice in VO_2max at generation 11 (Rezende et al. 2006a), though they have been reported to differ in later generations (Hiramatsu et al. 2017) and in total distance run (Garland, 2003; Houle-Leroy et al. 2003), though mini-muscle mice run faster than mice without the phenotype in later generations (Dlugosz et al. 2009). Thus, they would not be predicted to differ from other mice in nutrient canal area. In fact, no significant differences were found in total nutrient canal area or in number between normal mice and those possessing the mini-muscle phenotype (Figs 5E and 6E, Table 2).

Advantages of the methodology

Although descriptions of nutrient arteries and their foramina (on the external surface of long bones) have been

published previously (Greene, 1935; Rogers & Gladstone, 1950; Brookes & Harrison, 1957; Brookes, 1971; Henderson, 1978; Seymour et al. 2012; Allan et al. 2014), there are currently no precedents for modeling and quantifying the major vessels supplying blood to the skeleton, and very little is known about the morphology of, and potential variation in, the shapes of the canals themselves. A primary objective of this study was to develop a method to quantify accurately the morphology of nutrient canals, in particular their cross-sectional areas. In doing so, the method also helped reduce potential overestimation of nutrient canal area size that could be calculated due to the oblique orientation of the canal itself in the cortex. The use of μCT scans to visualize the nutrient canals *in situ* allowed us to document novel morphologies and branching patterns previously undescribed (Fig. 4). If the nutrient canal, and by extension the nutrient artery, showed little variation in diameter along its path from the periosteum to the medullary cavity, then measurements at the nutrient foramen opening would probably suffice to estimate blood flow to the bone. However, the nutrient canal shows considerable variation in both size and shape, and since blood flow through the nutrient artery is restricted by the smallest cross-sectional area of the vessel, as predicted by the Hagen–Poiseuille equation [$Q = (P\pi r^4)/(8L\eta)$], our virtual approach allowed us to obtain more realistic measures of the minimum cross-sectional area of the nutrient canal. Moreover, observations on all 137 femora demonstrated that the nutrient foramen itself was never the site of minimum cross-sectional area for the nutrient artery, and hence could not serve as a blood flow-limiting structure, thus confirming our need to take measurements from within the nutrient canal itself.

On the variability of nutrient canals

Although previous observations of nutrient foramina are limited, most describe a single nutrient artery penetrating long bones at a right angle to the long axis of the bone, developing an oblique orientation over time due to asymmetric bone growth, with no branching detected en route to the medullary cavity (Greene, 1935; Rogers & Gladstone, 1950; Brookes & Harrison, 1957; Brookes, 1958; Henderson, 1978; Singh et al. 1991). Variation in nutrient foramen number is not unknown, but anatomical descriptions of nutrient foramen have noted that although most long bones possess only one nutrient foramen, some may possess two, and some have none at all (Payton, 1934; Carroll, 1963; Campos et al. 1987). Despite the long history of external descriptions on nutrient arteries, and the foramina they leave behind, there has been no previous study which models the morphology of the nutrient canal.

Despite predictions of one to two canals per bone based on reports from the literature, in the 137 observations of this study, mice surprisingly averaged between four and five nutrient canals per femur. This difference may be partly the result of variations in interpretation of what constitutes a 'nutrient canal'; here we define a nutrient canal as a continuous absence of cortical bone breaching the periosteum and traversing to the medullary cavity of the femur in the area below the femoral neck and above the patellar groove (Figs 2 and 3). The condition that a nutrient canal must traverse the entirety of the cortical bone eliminates potential confusion with periosteal (external) vessels, and limiting the range of observations to the region between the femoral neck and patellar groove eliminates confusion with metaphyseal vessels found above and below this range. Although values for the total number of canals were not significantly correlated with selection history, sex or the mini-muscle phenotype (Fig. 6E, Table 2), the display of variability in nutrient canal structure is unprecedented (Fig. 4). Modeling of nutrient canals revealed an additional novelty in that nutrient arteries can, and occasionally do, branch within cortical bone. The findings of this study warrant meaningful, quantitative observations of nutrient canals in a broader range of organisms, to help move towards a broad understanding of the physiology behind the major vessels supplying blood to long bones.

Future directions

The generality of our findings should be thoroughly tested in representative members of a wider sample of taxa that vary in body size, locomotor activity, and metabolic rate. For *M. domesticus*, our results suggest that nutrient canal dimensions are related to locomotor activity. However, the mechanism of this relation has not been fully demonstrated. Correlation of individual activity and metabolic data to individual nutrient canal size would help to link the metabolic activity of an organism definitively to its skeletal properties, as would additional experimental manipulations of physical activity, such as housing animals with or without access to wheels during their development. Although the present study suggests that nutrient canal area can be related to metabolic activity, one should distinguish between the metabolic rate of an organism and that of its organs. The metabolic activity of the skeleton can be partitioned among the following functions: growth, bone modeling/remodeling, hematopoiesis, and mineral reservoir. The current contributions of each function to the specific metabolic rate of bone, as well as their contribution to an organism's overall metabolic rate, are unknown. However, it has been estimated that approximately 11% of total cardiac output is directed towards the skeleton under resting conditions (Gross et al. 1981). The large volume of blood supplied to the skeleton at rest may indicate that nutrient canal dimensions are more reflective of specific metabolic needs of bone as opposed to systemic cardiac output during exercise. As a result, insights into the relation between the metabolic actions of bone (bone growth, modeling/remodeling, and

mineral deposition/acquisition) and the major vasculature system supplying nutrients to feed those actions (nutrient vessels) open the possibility of gaining further inferences towards the physiology of extinct taxa, which would be a boon to both evolutionary physiology (Garland & Carter, 1994) and paleophysiology (e.g. Seymour et al. 2012).

Acknowledgements

We thank Dr. Roger S. Seymour for encouraging us to study nutrient canals. We thank Dr. Patricia A. Freeman for skeletonizing the mice. We thank the University of Southern California Molecular Imaging Center and their staff for assisting with the acquisition of μCT data. Invaluable discussion about this project was provided by Dr. Tomasz Owerkowicz and Dr. Stuart Sumida. This research was supported by both the Research Initiative for Research Enhancement and the Office of Graduate Studies at California State University San Bernardino, to N.S., and U.S. National Science Foundation grant DEB-1655362 to T.G. and BMMB-1436569 to A.H.

Author contributions

N.L.S. conceived and designed the research, designed the methodology used to acquire data, acquired the data, performed the analyses, and drafted and revised the manuscript. B.A.P. helped design the methodology for μCT scanning and data acquisition, and revised the manuscript. T.G. conceived, designed, and executed the protocol used to generate mice selectively bred for high voluntary wheel-running behavior, conceived and designed the research, provided the skeletal materials, assisted in data analysis, and revised the manuscript. A.M.H. conceived and designed the research, assisted in data analysis, and revised the manuscript.

References

Allan G, Cassey P, Snelling E, et al. (2014) Blood flow for bone remodelling correlates with locomotion in living and extinct birds. *J Exp Biol* **217**, 2956–2962.

Brookes M (1958) The vascular architecture of tubular bone in the rat. *Anat Rec* **132**, 25–47.

Brookes M (1971) *The Blood Supply of Bone*. London: Appleton-Century-Crofts.

Brookes M, Harrison R (1957) The vascularization of the rabbit femur and tibiofibula. *J Anat* **91**, 61–74.

Campos F, Pellico G, Alias G, et al. (1987) A study of the nutrient foramina in human long bones. *Surg Radiol Anat* **9**, 251–255.

Carano R, Filvaroff E (2003) Angiogenesis and bone repair. *Drug Discov Today* **8**, 980–989.

Carroll S (1963) A study of the nutrient foramina of the humeral diaphysis. *J Bone Joint Surg Br* **45B**, 176–181.

Castro A, Garland T Jr (2018) Evolution of hindlimb bone dimensions and muscle masses in house mice selectively bred for high voluntary wheel-running behavior. *J of Morphol* **279**, 766–779.

Copes L, Schutz H, Dlugosz E, et al. (2015) Effects of voluntary exercise on spontaneous physical activity and food consumption in mice: results from an artificial selection experiment. *Physiol Behav* **149**, 86–94.

Devlin M, Lieberman D (2007) Variation in estradiol level affects cortical bone growth in response to mechanical loading in sheep. *J Exp Biol* **210**, 602–613.

Dlugosz E, Chappell M, McGillivray D, et al. (2009) Locomotor trade-offs in mice selectively bred for high voluntary wheel running. *J Exp Biol* **212**, 2612–2618.

Dlugosz E, Schutz H, Meek T, et al. (2013) Immune response to a *Trichinella spiralis* infection in house mice from lines selectively bred for high voluntary wheel running. *J Exp Biol* **216**, 4212–4221.

Eliakim A, Raisz L, Brasel J, et al. (1997) Evidence for increased bone formation following a brief endurance-type training intervention in adolescent males. *J Bone Miner Res* **12**, 1708–1713.

Frost H (1987) Bone 'mass' and the 'mechanostat': a proposal. *Anat Rec* **219**, 1–9.

Garland T Jr (2003) Selection experiments: an under-utilized tool in biomechanics and organismal biology. In:*Vertebrate Biomechanics and Evolution*, (eds Bels VL, Gasc J-P, Casinos A) pp. 23–56. Oxford: BIOS Scientific Publishers Limited.

Garland T Jr, Carter P (1994) Evolutionary physiology. *Annu Rev Physiol* **56**, 579–621.

Garland T Jr, Freeman P (2005) Selective breeding for high endurance running increases hindlimb symmetry. *Evolution* **59**, 1851.

Garland T Jr, Morgan M, Swallow J, et al. (2002) Evolution of a small-muscle polymorphism in lines of house mice selected for high activity levels. *Evolution* **56**, 1267–1275.

Garland T Jr, Kelly S, Malisch J, et al. (2011) How to run far: multiple solutions and sex-specific responses to selective breeding for high voluntary activity levels. *Proc R Soc B Biol Sci* **278**, 574–581.

Girard I, Garland T Jr (2002) Plasma corticosterone response to acute and chronic voluntary exercise in female house mice. *J Appl Physiol* **92**, 1553–1561.

Girard I, McAleer M, Rhodes J, et al. (2001) Selection for high voluntary wheel-running increases speed and intermittency in house mice (*Mus domesticus*). *J Exp Biol* **204**, 4311–4320.

Greene E (1935) Anatomy of the rat. *Trans Am Philos Soc* **27**, ii.

Gross P, Marcus M, Heistad D (1981) Measurements of blood flow to bone and marrow in experimental animals by means of the microsphere technique. *J Bone Joint Surg Am* **63A**, 1028–1031.

Henderson R (1978) The position of the nutrient foramen in the growing tibia and femur of the rat. *J Anat* **125**, 593–599.

Hiramatsu L, Kay J, Thompson Z, et al. (2017) Maternal exposure to Western diet affects adult body composition and voluntary wheel running in a genotype-specific manner in mice. *Physiol Behav* **179**, 235–245.

Houle-Leroy P, Guderley H, Swallow J, et al. (2003) Artificial selection for high activity favors mighty mini-muscles in house mice. *Am J Physiol Regul Integr Comp Physiol* **284**, R433–R443.

Katsimbri P (2017) The biology of normal bone remodelling. *Eur J Cancer Care (Engl)* **26**, e12740.

Kelly S, Czech P, Wight J, et al. (2006) Experimental evolution and phenotypic plasticity of hindlimb bones in high-activity house mice. *J Morphol* **267**, 360–374.

Kelly S, Bell T, Selitsky S, et al. (2013) A novel intronic single nucleotide polymorphism in the Myosin heavy polypeptide 4 gene is responsible for the mini-muscle phenotype characterized by major reduction in hind-limb muscle mass in mice. *Genetics* **195**, 1385–1395.

Knothe Tate M (2003) 'Whither flows the fluid in bone?' An osteocyte's perspective. *J Biomech* **36**, 1409–1424.

Kolb E, Kelly S, Middleton K, et al. (2010) Erythropoietin elevates VO_2max but not voluntary wheel running in mice. *J Exp Biol* **213**, 510–519.

Lieberman DE (2003) Optimization of bone growth and remodeling in response to loading in tapered mammalian limbs. *J Exp Biol* **206**, 3125–3138.

Malisch JL, Saltzman W, Gomes FR, et al. (2006) Baseline and stress-induced plasma corticosterone concentrations of mice selectively bred for high voluntary wheel running. *Physiol Biochem Zool* **80**, 146–156.

Malisch J, Breuner C, Kolb E, et al. (2009) Behavioral despair and home-cage activity in mice with chronically elevated baseline corticosterone concentrations. *Behav Genet* **39**, 192–201.

Meek T, Lonquich B, Hannon R, et al. (2009) Endurance capacity of mice selectively bred for high voluntary wheel running. *J Exp Biol* **212**, 2908–2917.

Middleton KM, Shubin CE, Moore DC, et al. (2008) The relative importance of genetics and phenotypic plasticity in dictating bone morphology and mechanics in aged mice: evidence from an artificial selection experiment. *Zoology* **111**, 135–147.

Payton C (1934) The position of the nutrient foramen and direction of the nutrient canal in the long bones of the madder-fed pig. *J Anat* **68**, 500–510.

Pearson O, Lieberman D (2004) The aging of Wolff's 'law': ontogeny and responses to mechanical loading in cortical bone. *Am J Phys Anthropol* **125**, 63–99.

Rector R, Rogers R, Ruebel M, et al. (2008) Participation in road cycling vs running is associated with lower bone mineral density in men. *Metabolism* **57**, 226–232.

Rezende E, Garland T Jr, Chappell M, et al. (2006a) Maximum aerobic performance in lines of *Mus* selected for high wheel-running activity: effects of selection, oxygen availability and the mini-muscle phenotype. *J Exp Biol* **209**, 115–127.

Rezende E, Gomes F, Malisch J, et al. (2006b) Maximal oxygen consumption in relation to subordinate traits in lines of house mice selectively bred for high voluntary wheel running. *J Appl Physiol* **101**, 477–485.

Rhinelander F (1972) Circulation in bone. In: *The Biochemistry and Physiology of Bone*, (eds Bourne G) pp. 1–77. New York: Academic Press.

Robling A, Warden S, Shultz K, et al. (2007) Genetic effects of bone mechanotransduction in congenic mice harboring bone size and strength quantitative trait loci. *J Bone Miner Res* **22**, 984–991.

Rogers W, Gladstone H (1950) Vascular foramina and arterial supply of the distal end of the femur. *J Bone Joint Surg Am* **32A**, 867–874.

Rubin C, Lanyon L (1984) Regulation of bone formation by applied dynamic loads. *J Bone Joint Surg Am* **66**, 397–402.

Schirrmacher K, Lauterbach S, Bingmann D (1997) Oxygen consumption of calvarial bone cells in vitro. *J Orthop Res* **15**, 558–562.

Seymour R, Smith S, White C, et al. (2012) Blood flow to long bones indicates activity metabolism in mammals, reptiles and dinosaurs. *Proc R Soc B Biol Sci* **279**, 451–456.

Sim F, Kelly P (1970) Relationship of bone remodeling, oxygen consumption, and blood flow in bone. *J Bone Joint Surg Am* **52**, 1377–1389.

Singh I, Sandhu H, Herskovits M (1991) Bone vascularity. In: *Bone Matrix and Bone Specific Products*, (eds Hall B) pp. 141–157. Boca Raton: CRC Press.

Swallow J, Carter P, Garland T Jr (1998a) Artificial selection for increased wheel-running behavior in house mice. *Behav Genet* **28**, 227–237.

Swallow J, Garland T Jr, Carter P, et al. (1998b) Effects of voluntary activity and genetic selection on aerobic capacity in house mice (*Mus domesticus*). *J Appl Physiol* **84**, 69–76.

Swallow J, Koteja P, Carter P, et al. (1999) Artificial selection for increased wheel-running activity in house mice results in decreased body mass at maturity. *J Exp Biol* **202**, 2513–2520.

Swallow J, Koteja P, Carter P, et al. (2001) Food consumption and body composition in mice selected for high wheel-running activity. *J Comp Physiol B* **171**, 651–659.

Syme D, Evashuk K, Grintuch B, et al. (2005) Contractile abilities of normal and 'mini' triceps surae muscles from mice (*Mus domesticus*) selectively bred for high voluntary wheel running. *J Appl Physiol* **99**, 1308–1316.

Trueta J (1964) The role of the vessels in osteogenesis. *Plast Reconstr Surg* **33**, 206.

Trueta J (1974) Blood supply and the rate of healing of tibial fractures. *Clin Orthop* **105**, 11–26.

Wallace I, Middleton K, Lublinsky S, et al. (2010) Functional significance of genetic variation underlying limb bone diaphyseal structure. *Am J Phys Anthropol* **143**, 21–30.

Wallace I, Tommasini S, Judex S, et al. (2012) Genetic variations and physical activity as determinants of limb bone morphology: an experimental approach using a mouse model. *Am J Phys Anthropol* **148**, 24–35.

Supporting Information

Additional supporting information may be found online in the Supporting Information section at the end of the article.

Fig. S1. Virtual rendering of a nutrient canal with non-linear (i.e. curved) path from the periosteal surface to endosteal surface.

Fig. S2. Virtual rendering of a nutrient canal that contains a bifurcated path within the cortical bone.

Table S1. Preliminary two-way nested analysis of covariance models of femoral nutrient canal dimensions and counts; results shown only for potential covariates.

Supporting Information

Additional supporting information may be found in the online version of this article:

Table S1 Preliminary two-way nested analysis of covariance models of femoral nutrient canal dimensions and counts.

Fig. S1 Illustration of the protocol used to measure minimum cross-sectional area of a curved nutrient canal.

Fig. S2 Illustration of the protocol used to measure minimum cross-sectional area of a branched nutrient canal.

Supplemental Table S1 Preliminary two-way nested analysis of covariance models of femoral nutrient canal dimensions and counts; results shown only for potential covariates.

		Body Mass			Body Length			Femur Length		
Variable	N	df	F	P	df	F	P	df	F	P
Proximal Area (mm^2)	133	1, 6	2.74	0.1009	1, 6	1.00	0.3203	1, 6	2.13	0.1476
Distal Area (mm^2)	134	1, 6	0.05	0.8176	1, 6	0.03	0.8526	1, 6	1.03	0.3133
Total Area (mm^2)	134	1, 6	0.32	0.5710	1, 6	0.15	0.6999	1, 6	0.00	0.9600
Proximal Number	137	1, 6	1.34	0.2496	1, 6	0.17	0.6769	1, 6	1.09	0.2984
Distal Number	137	1, 6	0.07	0.7918	1, 6	0.04	0.836	1, 6	0.25	0.6148
Total Number	137	1, 6	0.34	0.5603	1, 6	0.18	0.6715	1, 6	1.18	0.2787

In preliminary analyses, a nested analysis of covariance was performed for all canal traits with body mass, body length, or femur length identified as potential covariates. None of these covariates were ever statistically significant, so they were removed from final models.

Supplemental Figure S1 Virtual rendering of a nutrient canal with non-linear (i.e. curved) path from the periosteal surface to endosteal surface. To identify the canal's minimum cross-sectional area, the canal was virtually reoriented in Amira software at several points where major changes in curvature (assessed visually) occurred so that multiple perpendicular cross-sections could be obtained along the path of the curved canal. The cross-sectional area was measured for each new section, but only the cross-section with the smallest calculated area was ultimately used for subsequent analyses.

Supplemental Figure S2 Virtual rendering of a nutrient canal that contains a bifurcated path within the cortical bone. The black solid line indicates the cross-section taken from source trunk at its narrowest point, while black dashed lines indicate cross-sections taken from branches at their narrowest points. Cross-sectional area was measured for all three sections. If the sum of the minimum cross-sectional areas of the branches was greater than their source trunk, then the branches were not considered to be blood flow limiting structures and were ignored, while only the trunk was recorded. If the cross-sectional area of the source trunk was greater than the sum of its branches, then the branches were the blood-flow limiting structures and both branches counted as distinct nutrient canals, while the trunk was ignored.

Supplemental Figure S1

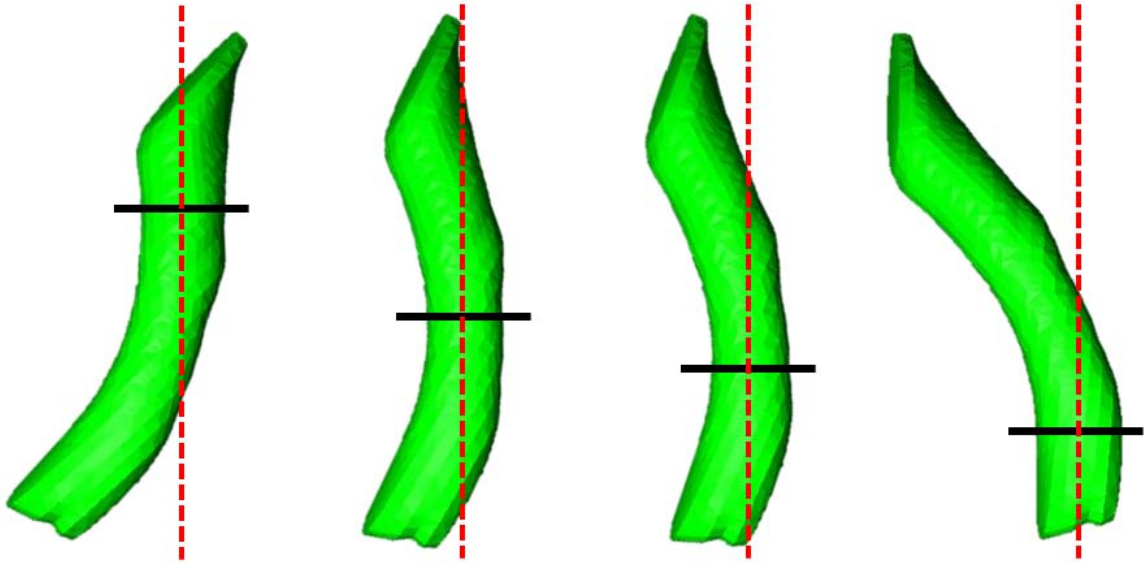

Supplemental Figure S2